Journal of Environmental Radioactivity 298 (2026) 108110

Contents lists available at ScienceDirect

Journal of Environmental Radioactivity

journal homepage: www.elsevier.com/locate/jenvrad

# $^{137}$Cs in glacial meltwater on King George Island, maritime Antarctica

Michał Saniewski[a,*], Katarzyna Fudala[b], Robert Bialik[b,d], Bartłomiej Kola[c], Dominika Saniewska[d]

[a] Institute of Meteorology and Water Management – National Research Institute, Waszyngtona 42, Gdynia, 81-342, Poland
[b] Institute of Biochemistry and Biophysics, Polish Academy of Sciences, Pawińskiego 5a, Warsaw, Poland
[c] Department of Electronics and Information Technology, Institute of Electronic Systems, Warsaw University of Technology, Warsaw, Poland
[d] Faculty of Oceanography and Geography, University of Gdansk, Al. Marszałka Piłsudskiego 46, Gdynia, 81-378, Poland

ARTICLE INFO

*Keywords:*
$^{137}$Cs
Glacier meltwater
Maritime Antarctica
King George Island

ABSTRACT

Glacierised catchments in maritime Antarctica can retain deposited atmospheric $^{137}$Cs and remobilize it during seasonal melting. $^{137}$Cs activity was determined in meltwater from 12 glacier outlets on King George Island (South Shetland Islands) during the austral melt season using ammonium phosphomolybdate (AMP) pre-concentration and gamma spectrometry. Activities were very low: six outlets were below the detection limit (<0.08-0.09 Bq m$^{-3}$), whereas detectable values ranged from 0.12 ± 0.07 to 0.37 ± 0.07 Bq m$^{-3}$. Suspended sediment was recovered from three visibly turbid outlets and analysed separately. Sediment-associated $^{137}$Cs was low and heterogeneous among grain-size fractions, with the highest activity measured in the <0.63 mm fraction from Penderecki Glacier (1.21 ± 0.31 Bq kg$^{-1}$). In sediment-rich outlets, the particulate fraction contributed substantially to total $^{137}$Cs activity per unit volume of runoff, indicating that suspended material can act as a local carrier of fallout-derived $^{137}$Cs.

## 1. Introduction

In the Northern Hemisphere, global fallout from atmospheric nuclear weapons testing reached its maximum in 1963, following the intensive test series of 1961–1962. In Antarctica, however, the fallout signal was lower and delayed because radionuclides were transported to high southern latitudes mainly through interhemispheric and stratospheric circulation. Antarctic snow and ice-core records commonly show two artificial-radioactivity reference horizons, around 1955 and 1965, with the main $^{137}$Cs maximum and the mean deposition time centred around 1965 (Pourchet et al., 2003; Delmas et al., 2004). Despite this, $^{137}$Cs remains detectable in Antarctic environmental matrices, demonstrating that even remote polar regions were affected by anthropogenic radionuclide contamination (Schuller et al., 2002). Estimates of $^{137}$Cs deposition in Antarctica are highly variable and depend on the region and type of environmental material analysed. This variability is consistent with the global fallout pattern summarised by UNSCEAR (2000) and is also evident in Antarctic-specific studies. Soil-based estimates from the South Shetland Islands and Antarctic Peninsula are approximately 240-260 Bq m$^{-2}$ (Roos et al., 1994; Godoy et al., 1998), whereas snow and ice-core records compiled by Pourchet et al. (2003) indicate lower continent-scale values, ranging from 16 to 181 Bq m$^{-2}$, with a mean of 64 ± 32 Bq m$^{-2}$ and a median of 56 Bq m$^{-2}$.

King George Island, part of the South Shetland Archipelago (~62°S), is >90% ice-covered (1127 km$^2$). This area is characterized by high precipitation, a maritime climate, and extensive glaciation, resulting in strong seasonal meltwater outflows during the austral summer (Sanders et al., 2010; Ferreira et al., 2013). These conditions favor the atmospheric deposition, accumulation, and subsequent redistribution of radionuclides within this environment. Glaciers act as long-term sinks of atmospheric $^{137}$Cs, where the radionuclide becomes incorporated into snow and ice layers, only to be remobilized decades later through glacial melt and runoff (Saniewski et al., 2023a, 2023b). Over the past decades, the region's warming has accelerated the retreat and thinning of glaciers. At the island scale, glacier coverage decreased by about 10% between 1989 and 2020, and marine-terminating glaciers were estimated to account for 35% of the total glacier area lost (Rojas-Macedo et al., 2025). Within the Admiralty Bay protected area (ASPA-128), mapping shows that 6.1 km$^2$ of ice was lost from an initial 19.8 km$^2$ glaciated area between 1979 and 2018, corresponding to an approximately 31% reduction relative to 1979 (Pudełko et al., 2018).

* Corresponding author.
*E-mail address:* michal.saniewski@imgw.pl (M. Saniewski).

https://doi.org/10.1016/j.jenvrad.2026.108110
Received 8 March 2026; Received in revised form 5 June 2026; Accepted 17 July 2026
Available online 20 July 2026

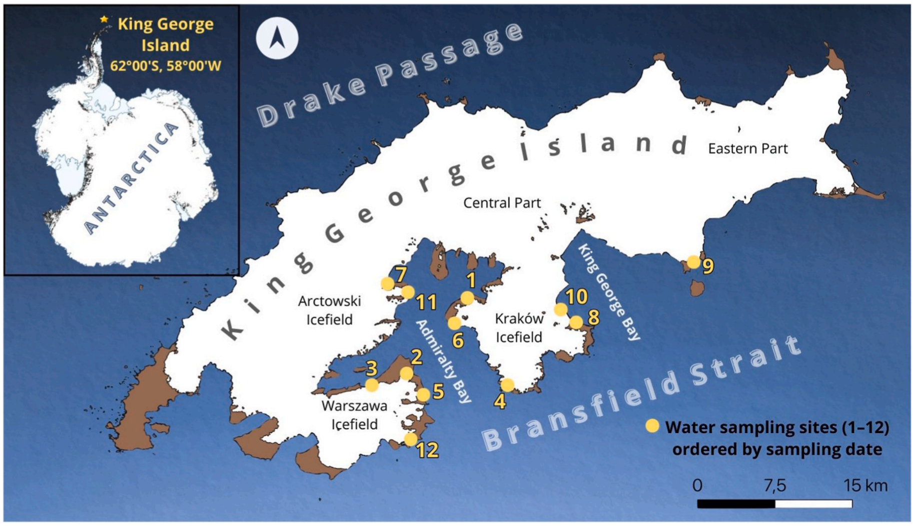


**Fig. 1.** Sampling locations on King George Island.

## 2. Material and methods

### 2.1. Study area and sampling

A total of 60 L of meltwater was collected from each of 12 selected glaciers on King George Island. Sampling was conducted as close as possible to the glacier termini, between 25 January 2024 and 2 March 2024 (Fig. 1). Because glacier termini and drainage systems on the island are highly dynamic, several glacier names used in the field are informal or locally adopted. Therefore, each sampling site is additionally reported with its GLIMS ID, providing a standardized reference to glacier outlines in the Global Land Ice Measurements from Space (GLIMS) database.

The physicochemical parameters of water were measured immediately after the samples reached the field station laboratory. Due to logistical constraints and the often-limited discharge of meltwater streams, in situ measurements of pH and specific conductivity were not feasible at all sites. Measurements were performed within 1–2 h using a YSI Pro 1030 multiparameter probe with automatic temperature compensation. For this reason, pH and specific conductivity were used only as supporting descriptors of meltwater chemistry, and no quantitative interpretation of $^{137}$Cs mobility was based on these parameters.

### 2.2. Laboratory analysis ($^{137}$Cs)

After measurement of physicochemical parameters, visibly turbid samples from the Ecology, Dera and Penderecki glaciers were allowed to settle for 12 h in the dark at approximately 5 °C. The supernatant was carefully decanted, whereas the sediment fraction was frozen at −20 °C for subsequent analysis. Suspended particulate material was freeze-dried, weighed and separated by dry sieving into three grain-size fractions: <0.63 mm, 0.63-1 mm and >1 mm. Each fraction was weighed separately, and its contribution to the total suspended sediment mass was calculated. Organic matter content was determined by loss on ignition (LOI). Fraction-specific suspended sediment concentrations [kg m$^{-3}$] were calculated from the dry mass of each fraction and the meltwater volume. Particulate $^{137}$Cs activity per unit volume of meltwater [Bq m$^{-3}$] was calculated as the sum of the products of fraction-specific $^{137}$Cs activity [Bq kg$^{-1}$ dry sediment] and fraction-specific suspended sediment concentration.

[kg m$^{-3}$]. Following either the initial measurements (samples without visible sediment) or the settling step (turbid samples), each water sample was acidified with 300 mL of 37% HCl. A natural caesium carrier (20 mg) was added, followed by equilibration and addition of 10 g ammonium phosphomolybdate (AMP; $(NH_4)_3PO_4 \cdot 12MoO_3 \cdot xH_2O$). Caesium was sorbed onto AMP during 20 min of stirring. The AMP phase was separated by decantation (48 h) and filtration, dried for 24 h at 50 °C, and stored in airtight containers with silica gel until measurement. The $^{137}$Cs activity retained in the AMP phase was expressed per original meltwater volume. Gamma-spectrometric measurements were performed using an Extended Range Coaxial Ge detector (XtRa GX4018, Canberra; 40% relative efficiency; 1.8 keV resolution at the 1332 keV peak of 60Co) coupled to an 8192-channel analyser and GENIE 2000 software. The counting time was 240,000 s per sample. $^{137}$Cs activities were calculated from the net area of the 661.7 keV photopeak after background subtraction, efficiency correction, gamma-emission probability correction and decay correction to the sampling date. Efficiency calibration was performed using certified mixed gamma-emitting standards (BW/Z-63/19/20) prepared in cylindrical containers of the same counting geometry as the environmental samples. The standards covered the relevant energy range, including the 661.7 keV photopeak of $^{137}$Cs. Standards with different heights (1–25 mm) were used to account for variable sample thickness. Background spectra were measured separately and subtracted during spectrum analysis. For most AMP-preconcentrated meltwater samples, $^{137}$Cs activities were calculated using the AMP-based $^{137}$Cs calibration, because the final counting geometry corresponded to the available AMP calibration geometry. The AMP calibration was prepared specifically for the 661.7 keV photopeak of $^{137}$Cs. For the three visibly turbid samples from Ecology, Dera and Penderecki glaciers, marked with an asterisk in Table 1, the AMP-retained phase was treated separately from the recovered suspended sediment. In these samples, the dried AMP-retained phase still contained additional fine material, as indicated by a dry mass exceeding 10 g of the initially added AMP and by a final layer height deviating from the AMP calibration geometry. Therefore, the direct AMP calibration was not applied to these three samples. Their AMP-retained $^{137}$Cs activities were calculated using the height-specific liquid-standard efficiency calibration and corrected for AMP self-attenuation. The AMP self-attenuation correction factor was determined from paired recalculations of 30 L monitoring water samples processed using the same AMP preconcentration procedure. Each spectrum was recalculated using both the AMP-based $^{137}$Cs calibration and the corresponding liquid-standard calibration. The AMP/liquid activity ratio for the 661.7 keV photopeak was 1.15895 ± 0.00024 (mean ± SD; n = 72), with a median of 1.15892 and a range of 1.15836–1.15953. For Ecology, Dera and Penderecki, final AMP-retained activities were calculated as:

$$A_{final} = \text{Aliquid,height-specific} \times 1.15895.$$

**Table 1**
Physicochemical parameters and $^{137}$Cs activity in meltwater collected from glaciers on King George Island.

| No. | Glacier | Distance from the glacier front [m] | GLIMS ID | Sampling date | Meltwater: SPC [µS cm$^{-1}$] | pH | $^{137}$Cs [Bq m$^{-3}$] |
|---|---|---|---|---|---|---|---|
| 1 | Wanda | 76 | G301653E62114 S | 25.01.2024 | 168.7 | 7.11 | 0.27 ± 0.07 |
| 2 | Ecology[a] | 4 | G301512E62184 S | 27.01.2024 | 94.7 | 7.37 | 0.14 ± 0.07 |
| 3 | Dera[a] | 69 | G301446E62190 S | 27.01.2024 | 243.0 | 7.08 | 0.37 ± 0.07 |
| 4 | Penderecki[a] | 55 | G301731E62182 S | 01.02.2024 | 127.7 | 7.82 | 0.15 ± 0.10 |
| 5 | Sphinx | 500 | G301531E62191 S | 04.02.2024 | 125.4 | 6.39 | <0.09 |
| 6 | Vieville | 200 | G301692E62137 S | 07.02.2024 | 15.0 | 5.61 | 0.12 ± 0.07 |
| 7 | Domeyko | 90 | G301521E62059S | 08.02.2024 | 73.8 | 6.03 | <0.08 |
| 8 | White Eagle | 680 | G301850E62140 S | 09.02.2024 | 92.6 | 7.50 | <0.08 |
| 9 | Zbyszek | 570 | G302061E62067S | 17.02.2024 | 108.9 | 6.33 | <0.08 |
| 10 | Anna | 129 | G301782E62117 S | 22.02.2024 | 26.7 | 5.88 | <0.08 |
| 11 | Znosko | 69 | G301518E62100 S | 23.02.2024 | 113.9 | 6.06 | <0.08 |
| 12 | Windy | 413 | G301511E62218 S | 02.03.2024 | 63.1 | 7.47 | 0.22 ± 0.07 |

| No. | Glacier | Suspended sediment (subset): Sediment load [kg m$^{-3}$] | Grain size fraction [%] | | | $^{137}$Cs in sediment [Bq kg$^{-1}$] | | | Organic matter content [%] | | |
|---|---|---|---|---|---|---|---|---|---|---|---|
| | | | <0.63 mm | 0.63-1 mm | >1 mm | <0.63 mm | 0.63-1 mm | >1 mm | <0.63 mm | 0.63-1 mm | >1 mm |
| 2 | Ecology[a] | 0.73 | 35.1% | 62.3% | 2.6% | 0.22 ± 0.18 | 0.91 ± 0.22 | <0.24 | 7 | 8 | 0.8 |
| 3 | Dera[a] | 2.03 | 3.9% | 32.2% | 63.9% | <0.73 | 0.52 ± 0.16 | <0.18 | 8 | 9 | 0.8 |
| 4 | Penderecki[a] | 1.03 | 31.2% | 52.8% | 16.0% | 1.21 ± 0.31 | 0.26 ± 0.18 | <0.20 | 13 | 11 | 1.1 |

[a] Suspended sediment properties were measured only for the three glaciers marked with superscript 'a'.

Suspended-sediment fractions were measured as dry material in the same cylindrical counting geometry. Their $^{137}$Cs activities were calculated using the height-specific efficiency calibration corresponding to the measured sample thickness. Because this calibration was based on liquid standards, an additional conservative 10% relative uncertainty component was included to account for possible matrix-related effects in dry mineral material. This value was selected on the basis of external proficiency-test results for solid mineral matrices, in which the same routine laboratory procedure gave accepted $^{137}$Cs results for quartz sand and Japanese soil, with relative biases of −8.2% and −3.7%, respectively.

Minimum detectable activity (MDA) was calculated according to the Currie approach as $MDA = LLD/(t \cdot P\gamma \cdot \varepsilon \cdot q)$, where t is counting time, Pγ is gamma-emission probability, ε is detector efficiency, and q is the analysed sample quantity, expressed as dry mass for sediments or equivalent water volume for AMP-preconcentrated samples. The lower limit of detection was calculated as $LLD = 4.65\sqrt{Fc}$, where Fc is the Compton background area in the selected gamma-ray region at the 95% confidence level. All uncertainties reported for $^{137}$Cs activities represent combined standard uncertainties and include counting statistics, efficiency calibration, sample quantity and, where applicable, the additional matrix-related uncertainty component described above.

All reported $^{137}$Cs activities were decay-corrected to the sampling date listed in Table 1. The reliability, accuracy and comparability of the measurements were verified through participation in IAEA intercomparison exercises and national proficiency tests, including solid-matrix materials (IAEA-RML-2025-01 and IAEA-TERC-2025-01).

## 3. Results

Meltwater samples exhibited a broad range of physicochemical properties, whereas $^{137}$Cs activities were uniformly low: 6 of the 12 glaciers were below the limit of detection (LOD; <0.08–0.09 Bq m$^{-3}$), while the remaining sites showed low activities of 0.12 ± 0.07–0.37 ± 0.07 Bq m$^{-3}$ (Table 1). Suspended sediment loads in the three meltwater samples ranged from 0.73 to 2.03 kg m$^{-3}$. Dera had the highest sediment load and was dominated by > 1 mm material (63.9%), whereas Ecology and Penderecki were dominated by < 1 mm fractions. Sediment-associated $^{137}$Cs was low and heterogeneous among fractions, with the highest values measured in the <0.63 mm fraction from Penderecki (1.21 ± 0.31 Bq kg$^{-1}$) and in the 0.63-1 mm fraction from Ecology (0.91 ± 0.22 Bq kg$^{-1}$; Table 1).

## 4. Discussion

The activity of $^{137}$Cs in glacial waters on King George Island was low, ranging from values below the detection limit to a maximum of 0.37 ± 0.07 Bq m$^{-3}$ (Table 1). The low $^{137}$Cs activities measured in glacier runoff are consistent with the regional background in maritime Antarctica. Previous studies from King George Island showed that residual fallout remains detectable in seawater, sediments, soils, vegetation and biota, although generally at low levels (Saniewski et al., 2023a, 2023b). In Admiralty Bay, $^{137}$Cs was reported in seawater, sediments, microphytobenthos, zoobenthos and macrophytobenthos close to 1 Bq kg$^{-1}$ dw, whereas zoobenthic organisms ranged from 0.12 to 24.2 Bq kg$^{-1}$ dw (Saniewski et al., 2023a). Terrestrial data from King George Island also indicate that $^{137}$Cs is retained in soils and vegetation, with mean activities of 3.72, 3.70, 2.62, 4.07 and 2.08 Bq kg$^{-1}$ dw in lichens, bryophytes, vascular plants, soil and guano, respectively (Saniewski et al., 2023b). The measured $^{137}$Cs activity should therefore be interpreted as a combined runoff signal rather than as $^{137}$Cs released exclusively from glacier ice. Glacier runoff may remobilize $^{137}$Cs not only from snow and ice, but also from recently exposed proglacial soils, suspended particulate matter and forefield sediments. Consistent with this mixed-source interpretation, no clear effect of glacier terminus type was observed. The highest activities occurred at Dera (0.37 ± 0.07 Bq

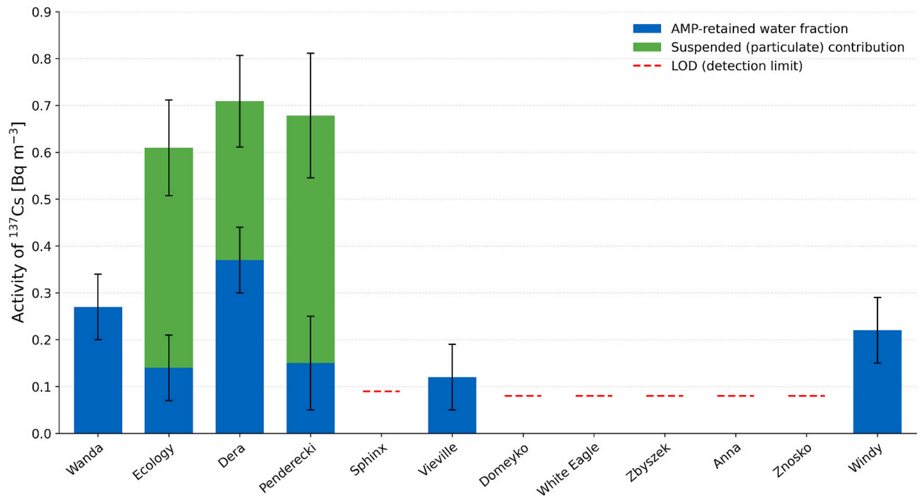


**Fig. 2.** Activity of $^{137}$Cs (Bq m$^{-3}$) in meltwater from glaciers of King George Island. The blue bars represent the dissolved fraction of $^{137}$Cs, while the green bars show the suspended (particulate) fraction. The red dashed line indicates the analytical limit of detection (LOD) in samples with $^{137}$Cs activity below LOD. (For interpretation of the references to colour in this figure legend, the reader is referred to the Web version of this article.)

m$^{-3}$), Wanda (0.27 ± 0.07 Bq m$^{-3}$) and Windy (0.22 ± 0.07 Bq m$^{-3}$), although these sites differed in sampling distance from the glacier front. Four of the six outlets with activities below the LOD were sampled at relatively greater distances from the termini. However, the detectable activity at Windy, collected approximately 400 m downstream, indicates that distance from the ice front alone did not control the measured signal (Table 1). The highest dissolved $^{137}$Cs activity and suspended sediment load were recorded at Dera glacier (Table 1), where the exported material was dominated by coarse particles (>1 mm), possibly reflecting stronger mechanical erosion and water-sediment interaction associated with its icefall morphology (Potocka et al., 2019). This pattern is consistent with the potential influence of sediment texture on dissolved-particulate partitioning, although radiocaesium is generally preferentially associated with fine and reactive particles (He and Walling, 1996; Singleton et al., 2017). Lower $^{137}$Cs activities were measured at the Ecology and Penderecki glaciers than at Dera glacier. These glaciers transported predominantly fine-grained sediments, with the coarsest fraction accounting for only 2.6% (Ecology) and 16% (Penderecki) of the total particulate matter (Table 1). The highest sediment-associated $^{137}$Cs activity was measured in the fine fraction from Penderecki glacier (1.21 ± 0.31 Bq kg$^{-1}$), which also had the highest LOI value (13%). In Ecology, the highest activity occurred in the 0.63-1 mm fraction (0.91 ± 0.22 Bq kg$^{-1}$), with LOI of 8%. These observations are consistent with the affinity of $^{137}$Cs for reactive fine or organic-rich particles, but the number of analysed sediment samples is too small to establish a quantitative relationship between grain size, organic matter and $^{137}$Cs activity. In the three sediment rich outlets where suspended material was recovered, the particulate fraction contributed substantially to the calculated total $^{137}$Cs activity per unit volume of runoff. This pattern remains site-specific because suspended sediment was analysed only for Ecology, Dera and Penderecki glaciers. The available data indicate that particulate transport can be important in sediment-rich meltwater, but the dataset is insufficient to generalise this partitioning to all glacier outlets on King George Island (Fig. 2).

At Wanda and Windy, where relatively high dissolved $^{137}$Cs activities were observed, suspended material was insufficient for grain-size separation and gamma-spectrometric analysis. Therefore, the dissolved particulate distribution could not be assessed. This further supports the interpretation that local drainage conditions and source mixing, rather than any single site parameter such as pH, conductivity or distance from the glacier front, controlled the measured $^{137}$Cs signal. Together with the particulate signal recorded at Ecology, Dera and Penderecki, these results indicate that suspended material may act as an important local carrier of fallout-derived $^{137}$Cs in sediment-rich glacier runoff.

## 5. Summary

$^{137}$Cs activity in glacier-fed runoff from King George Island was low and frequently below the detection limit, reflecting the low Antarctic fallout inventory, strong meltwater dilution and heterogeneous remobilisation within glacier and proglacial drainage systems. Differences among outlets were not clearly related to terminus type or sampling distance, indicating the importance of local drainage conditions and proglacial sediment interactions. In sediment-rich outlets, the particulate fraction contributed substantially to total $^{137}$Cs activity concentration, highlighting the role of suspended material in the local redistribution of fallout-derived $^{137}$Cs.

## CRediT authorship contribution statement

**Michał Saniewski:** Conceptualization, Formal analysis, Methodology, Visualization, Writing – original draft, Writing – review & editing. **Katarzyna Fudala:** Data curation, Investigation, Visualization, Writing – original draft, Writing – review & editing. **Robert Bialik:** Conceptualization, Data curation, Formal analysis, Writing – original draft, Writing – review & editing. **Bartłomiej Kola:** Data curation, Investigation, Writing – original draft, Writing – review & editing. **Dominika Saniewska:** Conceptualization, Visualization, Writing – original draft, Writing – review & editing.

## Declaration of competing interest

The authors declare that they have no known competing financial interests or personal relationships that could have appeared to influence the work reported in this paper.

## Acknowledgements

The authors would like to express their sincere gratitude to the Henryk Arctowski Polish Antarctic Station for logistical support. Special thanks are extended to the personnel of the 47th and 48th Polish Antarctic Expeditions for their invaluable assistance during fieldwork.

## Data availability

Data will be made available on request.

## References

Delmas, R.J., Beer, J., Synal, H.A., Muscheler, R., Petit, J.R., Pourchet, M., 2004. Bomb-test 36Cl measurements in Vostok snow (Antarctica) and the use of 36Cl as a dating tool for deep ice cores. Tellus B 56 (5), 492–498. https://doi.org/10.3402/tellusb.v56i5.16454.

Ferreira, P.A.L., Ribeiro, A.P., do Nascimento, M.G., Martins, C.C., de Mahiques, M.M., Montone, R.C., Figueira, R.C.L., 2013. 137Cs in marine sediments of Admiralty Bay. King George Island. Antarctica. Sci. Total Environ. 443, 505–510. https://doi.org/10.1016/j.scitotenv.2012.11.032.

Godoy, J.M., Schüttelkopf, H., Godoy, M.L.D.P., da Silva, P.S.C., 1998. Fallout radionuclides in Antarctica: accumulation in sediment and lichens. J. Environ. Radioact. 38 (2), 141–159.

He, Q., Walling, D.E., 1996. Interpreting particle size effects in the adsorption of 137Cs and unsupported 210Pb by mineral soils and sediments. J. Environ. Radioact. 30 (2), 117–137.

Potocka, M., Kidawa, A., Panasiuk, A., 2019. The effect of Glacier recession on benthic and pelagic communities: 509 case study in herve cove, Antarctica. JMSE 7, 285.

Pourchet, M., Magand, O., Frezzotti, M., Ekaykin, A., Winther, J.-G., 2003. Radionuclide deposition over Antarctica. J. Environ. Radioact. 68 (2), 137–158.

Pudełko, R., Angiel, P.J., Potocki, M., Jędrejek, A., Kozak, M., 2018. Fluctuation of glacial retreat rates in the Eastern part of warszawa icefield, King George Island, Antarctica, 1979–2018. Remote Sens. 10 (6), 892. https://doi.org/10.3390/rs10060892.

Rojas-Macedo, I., Bello, C., Suarez, W., Loarte, E., Vega-Jacome, F., Bustamante Rosell, M.G., Tapia, P.M., 2025. Using satellite imagery to assess glacier retreat in King George Island, Antarctica. Revista de Teledetección 65, 22317. https://doi.org/10.4995/raet.2025.22317.

Roos, P., Holm, E., Persson, R.B.R., Aarkrog, A., Nielsen, S.P., 1994. Deposition of 210Pb, 137Cs, 239+240Pu, 238Pu, and 241Am in the antarctic Peninsula area. J. Environ. Radioact. 24, 235–251.

Sanders, C.J., Santos, I.R., Patchineelam, S.R., Schaefer, C., Silva-Filho, E.V., 2010. Recent 137Cs deposition in sediments of Admiralty Bay. Antarctica. J. Environ. Radioact. 101 (6), 421–424.

Saniewski, M., Bałazy, P., Klajman, K., Saniewska, D., 2023a. Distribution of 137Cs in the marine environment from King George Island (Southern Shetlands. maritime Antarctica). Mar. Pollut. Bull. 197, 115752. https://doi.org/10.1016/j.marpolbul.2023.115752.

Saniewski, M., Wietrzyk-Pełka, P., Węgrzyn, M.H., Saniewska, D., Bałazy, P., Zalewska, T., 2023b. Distribution of 90Sr and 137Cs in biotic and abiotic elements of the coastal zone of the King George Island (South Shetland Archipelago, Antarctic Peninsula). Chemosphere 332, 138218. https://doi.org/10.1016/j.chemosphere.2023.138218.

Schuller, P., Bunzl, K., Voigt, G., Handl, J., Ellies, A., Castillo, A., 2002. Fallout radiocesium in an Antarctic region: deposition history. activity densities and vertical transport in soils. Radiat. Environ. Biophys. 41 (4), 295–302.

Singleton, A.A., Schmidt, A.H., Bierman, P.R., Rood, D.H., Neilson, T.B., Greene, E.S., Bower, J.A., Perdrial, N., 2017. Effects of grain size, mineralogy, and acid-extractable grain coatings on the distribution of the fallout radionuclides 7Be, 10Be, 137Cs, and 210Pb in River sediment. Geochem. Cosmochim. Acta 197, 71–86.

United Nations Scientific Committee on the Effects of Atomic Radiation, 2000. Sources and effects of ionizing radiation. UNSCEAR 2000 Report to the General Assembly, with Scientific Annexes. Volume I: Sources. United Nations, New York.